Characterization of excited states of ^{15}N through ^{14}C(p,p) ^{14}C using polarized proton beam

G. Murillo, M. Fernández, J. Ramírez, M.G. Mejia-Gil, R. Policroniades, and A. Varela
Instituto Nacional de Investigaciones Nucleares,

S.E. Darden† and S. Sen
University of Notre Dame, Notre Dame, IN, USA.

R.M. Prior
North Georgia College and State University, Georgia, USA.

E. Chávez
Instituto de Física, Universidad Nacional Autónoma de México.

Recibido el 10 de marzo de 2010; aceptado el 31 de agosto de 2010

Angular distributions of cross sections and analyzing powers were measured for ^{14}C(p, p)^{14}C for proton energies between 3.7 and 11.0 MeV in very small energy steps. A number of strong resonances are seen. Phase-shift analysis of the elastic scattering data yielded level parameters of eleven states in ^{15}N in the excitation energy region 13.7-21.0 MeV. Previous assignments of spin, parity and energy of levels are discussed.

Keywords: polarized proton beam; nuclear structure; elastic scattering.

Se midió la distribución angular de la sección eficaz diferencial y el poder analizador para la dispersión elástica de un haz de protones polarizados de entre 3.7 y 11 MeV de energía sobre ^{14}C con pasos muy finos. El análisis de los datos en términos de ondas parciales y corrimientos de fase de la matriz "S" nos permite deducir los números cuánticos y parámetros de diez estados del ^{15}N entre 13.7 y 21.0 MeV de energía de excitación. Las asignaciones previamente publicadas para estos niveles son discutidas.

Descriptores: Haz de protones polarizado; estructura nuclear; dispersión elástica.

PACS: 25.40.Cm; 27.20.+n; 29.27.Hj

1. Introduction

The details of the structure of the ^{15}N nucleus above 11 MeV of excitation energy are not well known, as is still the case for most nuclei. Except for the work of Weller *el al*. [1-3], data published to date in this energy range [1-6] provide limited information on the parameter values (spin, parity, energy and widths) of such levels. Previous polarization measurements [3,5] only show excitation curves in 100 keV steps with a ^{14}C target on a nickel backing. We have undertaken this study of elastic scattering of polarized protons from ^{14}C in order to improve the information of the levels structure of ^{15}N. We were able to determine the energy, spin and parity of eleven states. Agreement and differences with previously assigned values are presented.

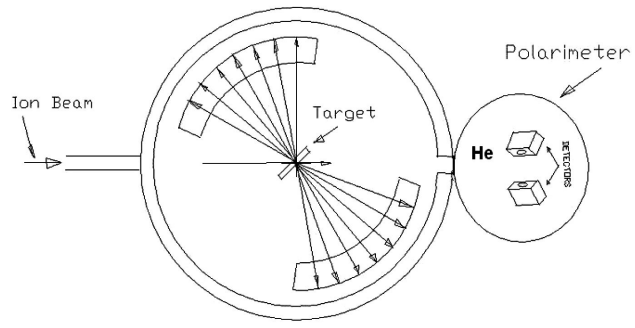

FIGURE 1. Schematic view of the experimental setup.

2. Experiment

The experimental procedure followed was similar to the one described in Refs. 7 and 8. A survey of the cross section was first carried out by measuring the excitation function at

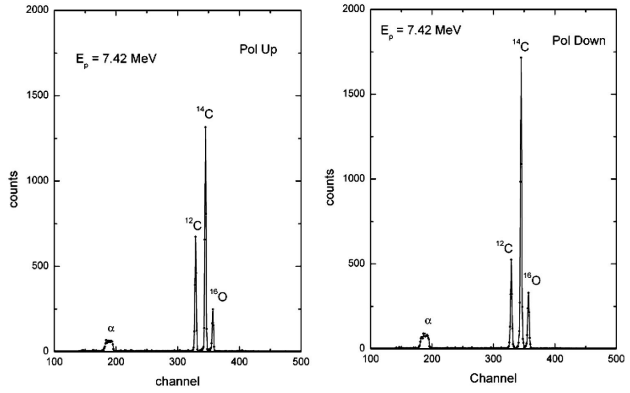

FIGURE 2. Raw energy spectra for protons with polarization up (left) and down (right) at 7.44 MeV. The detector was the one at 165° (backwards), at this angle the contribution from unwanted oxygen and carbon isotopes in the target can be easily separated. This information is used to correct the data at forward angles.

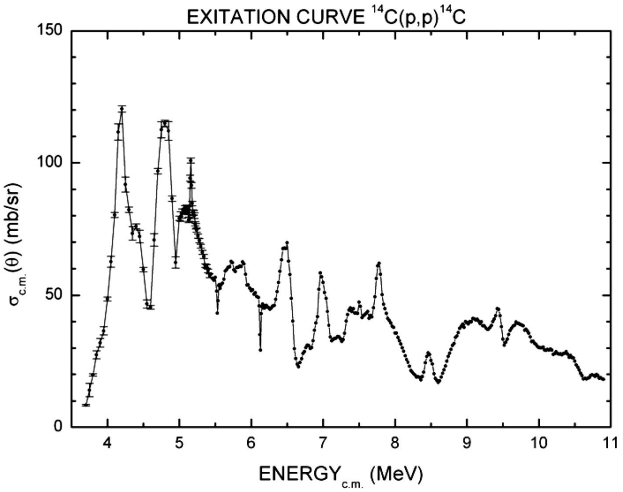

FIGURE 3. Excitation function for the ^{14}C(p,p)^{14}C elastic scattering. A continuous line is drawn just to better guide the eye.

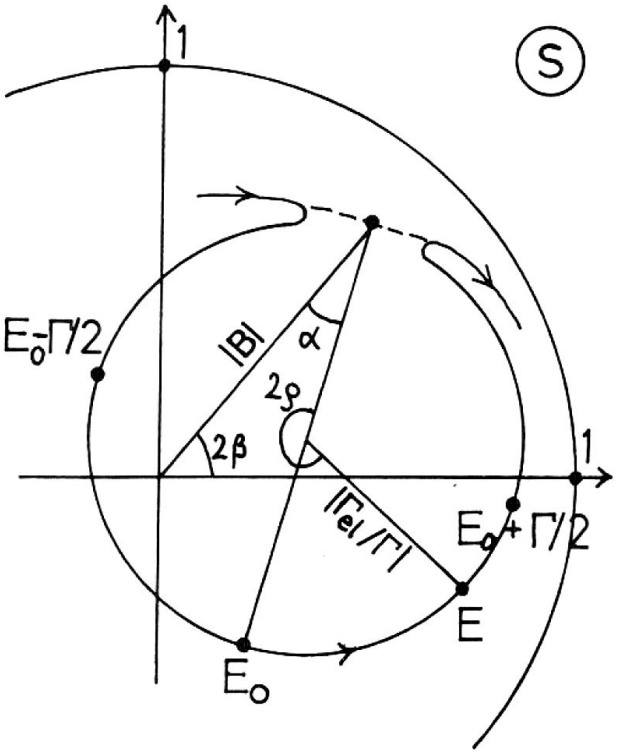

FIGURE 4. Theoretical Argand diagram showing the behavior of the phase shifts in the complex plane around a resonance. The parameters of the resonance are extracted from this kind of analysis.

several angles. These first measurements were carried out at the Tandem Accelerator Laboratory of the "Instituto Nacional de Investigaciones Nucleares" (Mexican nuclear research institute, ININ). Energy steps of 10 keV were used for proton energies between 4.8 and 9.0 MeV. The angular distribution of the differential cross section and the analyzing power were subsequently measured out at the University of Notre Dame using the polarized proton beam from the Lamb-shift ion source and the FN Tandem accelerator, The target was a 170 μg/cm^2 thick self-supported foil 90% enriched ^{14}C. ^{12}C and ^{16}O were the main contaminants in the target. Corrections had to be made to the elastic scattering data, especially at forward angles (35°, 45° and 55°). In order to get the absolute cross sections, detailed measurements were made with a non-polarized beam and a single detector to avoid normalization problems between 3.7 and 6.0 MeV at ININ. Figure 1 shows a schematic view of the experimental setup used at Notre Dame, the setup of the experiments at ININ consisted of just one single detector and no scheme is provided. Figure 2 shows a typical spectrum of protons at backward angles (165°) at E$_p$=7.42 MeV for the two modes of polarization (up and down). At these large angles, the elastic scattering peaks for ^{12}C, ^{14}C and ^{16}O are cleanly separated in the spectrum. Excitation function of the cross section for the elastic scattering are shown for θ_{lab}=165° in Fig. 3 in the full energy interval measured; in this figure, the line joining the data points does not represent any fit or calculation.

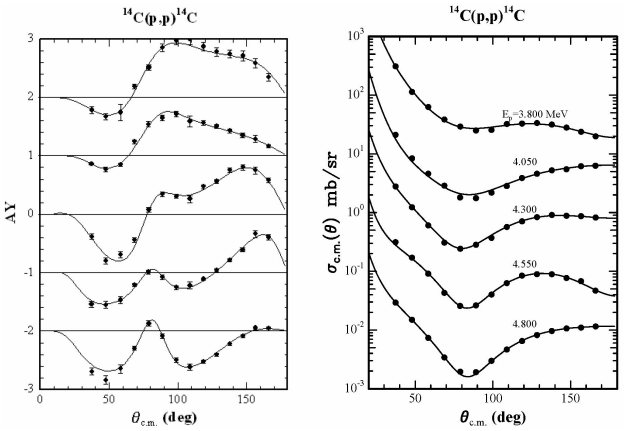

FIGURE 5. Angular distribution of analyzing power and differential cross section between 3.7 to 4.8 MeV. The error bars represent statistical errors. The solid lines are calculated form the result of the phase shift fit.

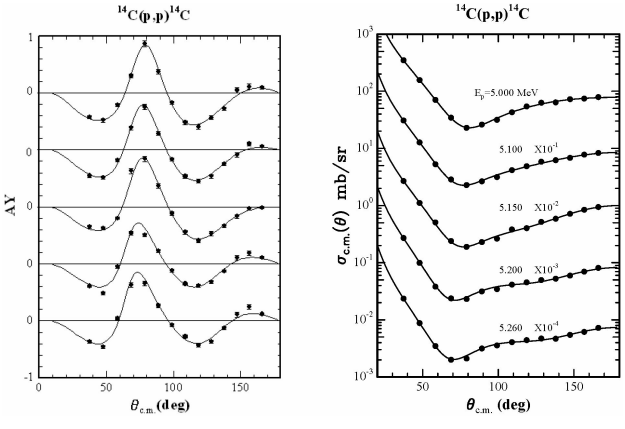

FIGURE 6. Angular distribution of analyzing power and differential cross section between 5.0 to 5.3 MeV. The error bars represent statistical errors. The solid lines are calculated form the result of the phase shift fit.

TABLE I. Excited states in ^{15}N from ^{14}C(p,p)^{14}C.

	This work					Weller				Ajzenberg		
	E_x	J_π	Γ_{cm}	Γ_p	Γ_{lab}	E_x	J_π	Γ_{lab}	Γ_p	E_x	J_π	Γ_{cm}
1	13.78	1/2+	735	385	788	13.82	1/2+	1000	500	13.9	1/2+	930
										13.99	5/2+	98
										14.09	(9/2+,7/2+)	22
										14.1	3/2+	100
										14.162	3/2(+)	27
2	14.13	5/2+	162	45	174	14.13	5/2+	105	25	14.24	5/2+	150
										14.38	7/2+	100
3	14.25	3/2+	1158	386	1242					14.4		1900
4	14.51	3/2-	151	66	162	14.50	3/2-	20	8	14.55		200
										14.647		33
										14.71		750
										14.72	5/2-	110
5	14.81	1/2-	67	18	72	14.72	3/2+	160	39	14.86		48
6	14.90	3/2-	50	4	54	14.94	3/2+	170	20	14.92		12
7	15.01	5/2+	39	4	42	15.04	3/2+	30	9	15.025		13
										15.09		80
										15.288		26
										15.373	13/2+	
8	15.37	1/2-	47	5	50	15.40	3/2-	42	12	15.38		75
										15.43		100
										15.45		750
										15.53		35
										15.6		95
										15.782		
9	15.93	5/2-	16	3	18					15.93		35
										15.944		21
										16.026		62
										16.19	3/2+	450
10	16.29	3/2-	223	86	248	16.27	3/2+	140	19	16.26	3/2+	150
										16.32		30
										16.39		44
										16.46		560
										16.576		27
										16.59	3/2-	490
11	16.72	3/2+	157	35	175	16.74	3/2+	140	17	16.677	1/2+	80

3. Analysis and results

The general procedure we have followed in the analysis of the data is similar to that used in previous studies [9,10]. A phase-shift analysis of the data is carried out over restricted energy intervals containing relatively few resonances and permitting a maximum of five phases to vary at a time. Once the resonances contributing to the elastic scattering have been identified and approximate levels parameters determined, the energy dependence of non-resonant phases and effects of nearby resonances are included in the calculations to provide more reliable level parameters.

When a phase shift is fitted to the data around a resonance, it describes a well known loop in the complex plane (Argand diagram) as a function of energy. Figure 4 shows the way in which parameters of the resonance are extracted (theoretically) from such diagrams.

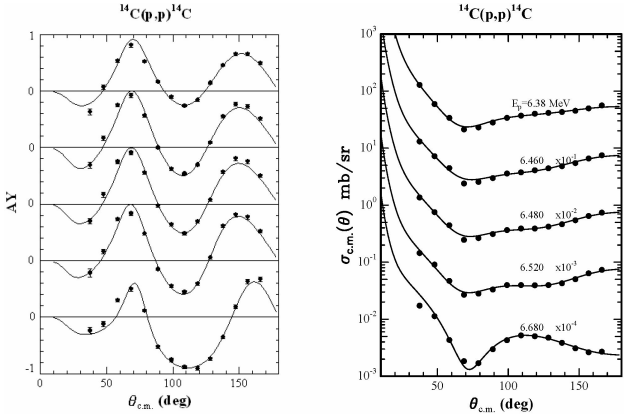

FIGURE 7. Angular distribution of analyzing power and differential cross section between 6.3 to 7.0 MeV. The error bars represent statistical errors. The solid lines are calculated form the result of the phase shift fit.

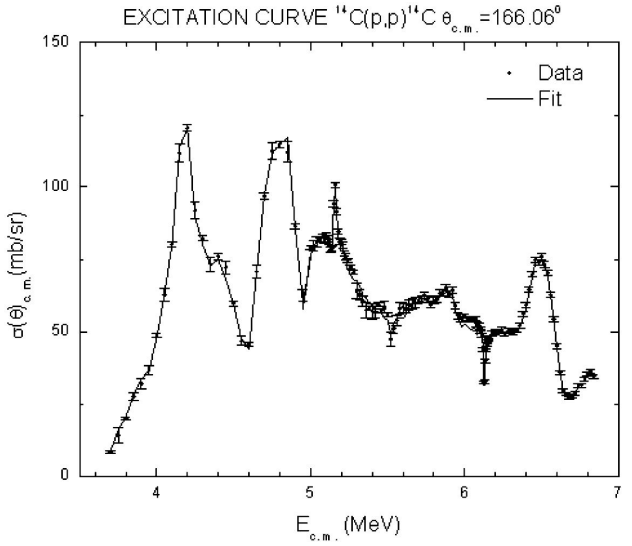

FIGURE 8. Excitation function for the ^{14}C(p,p)^{14}C elastic scattering between 6.3 to 7.0 MeV. The error bars represent statistical errors. The solid lines are calculated form the result of the phase shift fit.

In this work we will concentrate in the analysis of the data below 7 MeV. Figures 5, 6 and 7 show angular distributions in the energy region 3.7 - 7.0 MeV, the solid curves correspond to phase-shift fits. The phase shift fit to the excitation function for θ_{lab}=165° in the energy region of interest is shown in Fig. 8 as a solid curve.

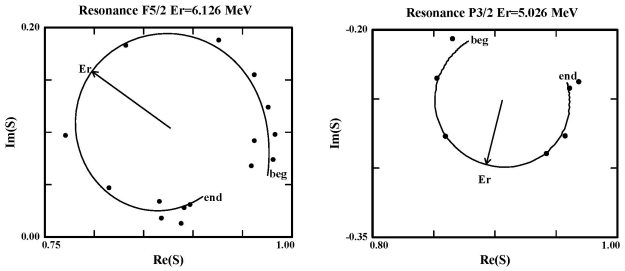

FIGURE 9. Example of Argand diagrams for the phase shift analysis of the data around two resonances: p3/2 at 5.026 MeV and f5/2 at 6.126 MeV.

The experimental phase shifts were fit by energy-dependent phases corresponding to scattering amplitude given by the Briet-Wigner expression. The search program FASTFIT [11] was employed to fit the expression to the phases. We obtained initial values for the parameters used in the calculations by drawing resonant circles through the experimental points in the Argand diagrams, and estimating resonance and background parameters for these trajectories. Figure 9 show examples of the Argand trajectories corresponding to case for which well-defined resonances behavior was observed, the solid line correspond to the FASFIT fit, and the arrow indicate the energy resonance for the level.

Table I summarizes the resonance parameters extracted from the calculations. Eleven resonant states in the energy range 3.7 - 7.0 MeV were identified.

4. Summary and conclusions

In this paper we report on the analysis of a fraction of a very large data set. We concentrate on the study of the most prominent resonant structure of the excitation function for the ^{14}C(p, p)^{14}C. Eleven resonant states in ^{15}N were identified. The use of polarized beams allows the full characterization of these states. With our results, we are able to correct or confirm previous assignments of spin, parity and width of all these states.

5. Acknowledgements

One of the authors (EC) wishes to acknowledge partial support to CONACYT under contract 51600 and DGAPAUNAM under contract: IN118310

†. Deceased

1. J.J. Ramírez, R.A. Blue, and H.R. Weller, *Phys. Rev. C* **5** (1972) 17.
2. H.R. Weller, R.A. Blue, J.J. Ramírez, and E.M. Bernstein, *Nucl. Phys. A* **207** (1973) 177.
3. H.R. Weller *et al.*, *Phys. Rev. C* 10 (1974) 575.
4. H.R. Weller, R.A. Blue, J.J. Ramírez, and E.M. Bernstein, *Phys. Rev. C* **11** (1975) 1464.
5. H.R. Weller, N.R. Roberson, D. Rickel, and D.R. Tilley, *Phys. Rev. Lett.* **33** (1974) 657.
6. M.H. Harakeh, P. Paul, H.M. Kuan and E.K. Warburton, *Phys. Rev. C* **12** (19775) 1410.

7. S.E. Darden *et al.*, *Nucl. Phys. A* **429** (1984) 218.
8. R.M. Prior, S.E. Darden, K.R. Nyga and H. Peatz gen, *Schiek, Nucl. Phys. A* **529** (1991) 190.
9. G. Murillo *et al.*, *Nucl. Phys. A* **318** (1979) 352.
10. M. Fernández *et al.*, *Nucl. Phys. A* **369** (1981) 425.
11. H.O. Meyer, W.G. Weitkamp, J.S. Dunham, T.A. Trainor and M.P. Baker, *Nucl. Phys. A* (1976) 269.
12. F. Ajzenberg-Selove, *Nuclear Physics A* **523** (1991) 1